Title	Antenna reconfiguration using metasurfaces
Author(s)	Zhu, H; Cheung, WSW; Yuk, TI
Citation	The 2014 Progress In Electromagnetics Research Symposium (PIERS 2014), Guangzhou, China, 25-28 August 2014. In PIERS Proceedings, 2014, p. 2400-2404
Issued Date	2014
URL	http://hdl.handle.net/10722/204116
Rights	Creative Commons: Attribution 3.0 Hong Kong License

Antenna Reconfiguration Using Metasurfaces

Hailiang Zhu, S. W. Cheung, and T. I. Yuk
Department of Electrical and Electronic Engineering
The University of Hong Kong, Hong Kong

Abstract— The paper describes the designs of a frequency-reconfigurable, polarization reconfigurable and pattern reconfigurable antennas using metasurfaces (MS). The frequency-reconfigurable and polarization reconfigurable antennas are composed of a simple circular patch antenna or slot antenna as the source antenna and a circular MS with the same diameter, with both source antenna and MS implemented using planar technology. The pattern reconfigurable antenna is composed of a circular patch antenna as the source antenna and a semicircular MS with the same diameter. In all these reconfigurable antennas, the MS is placed directly atop of the source antenna, making the antenna very compact and low profile with a thickness of only $0.05\lambda_0$. By rotating the MS around the center with respect to the source antenna, the frequency, polarization or pattern of the reconfigurable antenna can be reconfigured.

1. INTRODUCTION

In general, operating frequency, polarization and radiation pattern are the three major characteristics in the design of antennas. As the growing demand for integrating multiple wireless standards into a single wireless platform, it is highly desirable if one or more of the above mentioned performance characteristics in an antenna can be reconfigured. Thus substantial research work has been carried out to reconfigure these characteristics for antennas.

The mechanism used to reconfigure the operating frequency, polarization and radiation pattern of an antenna can be mechanical or electrical. Electrically reconfigurable antennas are far more popular and can be achieved by using PIN-diode switches or varactor diodes. In the design of these antennas, direct-current (DC) source and biasing circuits are needed to bias the PIN or varactor diodes. These electronic components and circuits may have adverse effects on the antennas performances such as efficiencies and radiation pattern. Moreover, the antenna performance depends on the reliability of the electronic components and the DC sources [1]. Mechanically reconfigurable antennas usually require adjusting some movable parts to achieve reconfiguration [2]. The main drawback is that the actuator used to produce the mechanical movements is very complicated and usually occupies much space, making it bulky and expensive. In fact, change of size and/or shape is the common problem for most mechanically reconfigurable antennas. To overcome these shortcomings, we propose to use metasurfaces to design reconfigurable antennas.

Metasurface (MS) is a two-dimensional equivalent of metamaterial and essentially a surface distribution of electrically small scatterers [3]. Due to its succinct planar structure and low cost, MS provides a good option for the movable part of mechanically reconfigurable antennas and can be easily integrated with printed planar antennas.

In this paper, we describe the use of MS to design three different types of reconfigurable antennas, namely, frequency-reconfigurable, polarization-reconfigurable and pattern-reconfigurable antennas. The frequency-reconfigurable and polarization reconfigurable antennas have been introduced in our previous papers [6, 7] in details and the idea of pattern reconfigurable antenna using MS is first time presented.

2. ANTENNAS DESIGN

2.1. Frequency-reconfigurable Antenna

The frequency-reconfigurable metasurfaced (FRMS) antenna described here, as shown in Fig. 1, consists of a patch antenna (as the source antenna) and a MS which uses a rectangular loop as the unit cell [6]. The patch antenna and MS are designed to have a circular shape with same diameter. The patch antenna is designed on a double-sided substrate using planar technology as shown in Fig. 1(a), while the MS is designed on a single-sided substrate, as shown in Figs. 1(b) and (c). The frequency reconfigurability of the antenna is achieved by rotating the MS around the center relative to the patch antenna. The rotation angle θ_R is measured from the y-axis as shown in Fig. 1(b). Due to the horizontal and vertical symmetries of the MS, $\theta_R = -\theta_R$ and the maximum rotation angle without repeating is 90°. In assembling the FRMS antenna, the non-copper side of the MS is

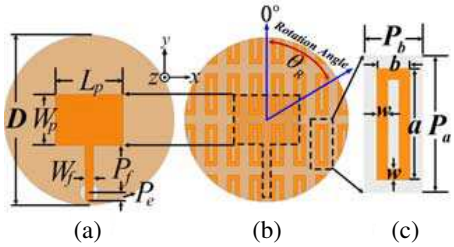

Figure 1: Geometries of (a) patch antenna, (b) MS and (c) unit cell.

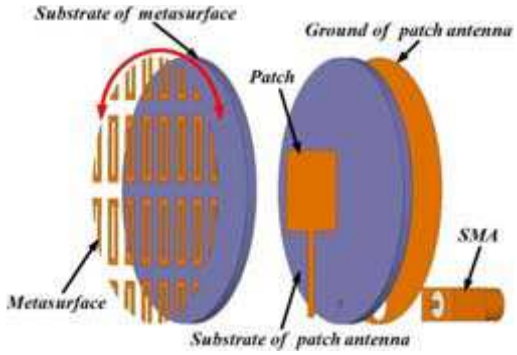

Figure 2: Assembly schematic of FRMS antenna.

Table 1: Dimensions of FRMS antenna (Unit: mm).

$\mathbf{P_a}$	$\mathbf{P_b}$	**a**	**b**	**w**	$\mathbf{L_p}$	$\mathbf{W_p}$	$\mathbf{W_f}$	$\mathbf{P_f}$	$\mathbf{P_e}$	**D**
12.4	5.4	10	3	1	16	12	2	11	2	40

placed in direct contact with the radiator of the patch antenna as shown in Fig. 2, leading to a very compact and low profile structure. The antenna is designed on the Rogers substrates RO4350B, having a thickness of 1.524 mm and a relative permittivity of $\varepsilon_r = 3.48$. The optimized dimensions are listed in Table 1.

2.2. Polarization Reconfigurable Antenna

The polarization-reconfigurable metasurfaced (PRMS) antenna, as shown in Fig. 3, consists of a slot antenna (as the source antenna) and a metasurface (MS) [7]. The MS is composed of corner-truncated square unit cells as shown in Fig. 3(a) on a single-sided substrate. The polarization reconfigurablity of the antenna is accomplished by rotating the MS around the center relative to the slot antenna. The rotation angle θ_R is measured from the y-axis as shown in Fig. 3(a). Studies have shown that with $\theta_R = 0°$ and 90°, the operation of the antenna is left-hand circular polarization (LHCP) and right-hand circular polarization (RHCP), respectively. With $\theta_R = 45°$ and 135°, the antenna is linearly polarized (LP) along the y-axis, same as that of the source antenna (the slot antenna). In assembling the PRMS antenna, the non-copper side of the MS is placed atop the slot antenna and is in direct contact with the feed-line (top side) of it as shown in Fig. 4. This leads to a very compact and low profile structure. An SMA connector is used to feed to the feed-line through the ground plane and the substrate material of the slot antenna. The dimensions of the final design are listed in Table 2.

2.3. Radiation Pattern Reconfigurable Antenna

The pattern reconfigurable metasurfaced antenna (PaRMS) is composed of a simple circular patch antenna and a semicircular MS with the same diameter, as shown in Figs. 5 and 6. The MS consists of small square patches used as the unit cells. Due to the semicircular structure of the MS, the

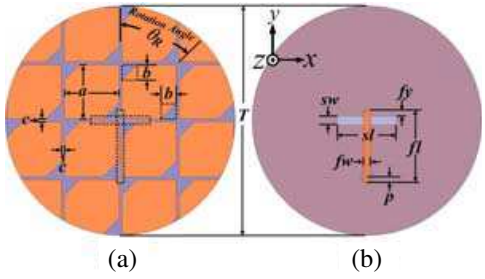

Figure 3: Geometries of (a) MS and (b) slot antenna.

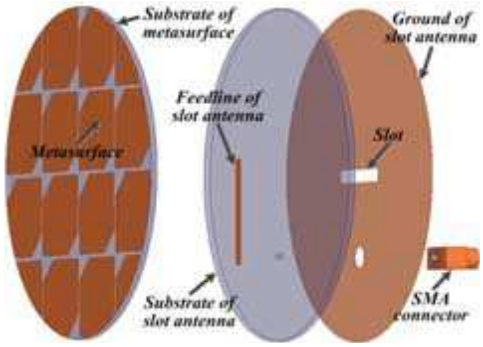

Figure 4: Assembly schematic of PRMS antenna.

integrated antenna will generate a tilted beam, making an angle of 30° with the boresight direction. By rotating the MS around the center of the antenna, the tilted beam can be steered to different directions. As the source antenna is circular and fed by a SMA connector at the center, the S_{11} of the PaRMS antenna is unchanged in rotation, thus simplifying the optimization work of the antenna significantly. The dimensions of the final design are listed in Table 3.

Table 2: Dimensions of PRMS antenna (Unit: mm).

a	b	c	sw	sl	fw	fl	fy	p	T
18.5	5.3	1	3	20	2.5	24.5	2	2	78

Table 3: Dimensions of PaRMS antenna (Unit: mm).

a	G	P_r	T
6	0.3	18	70

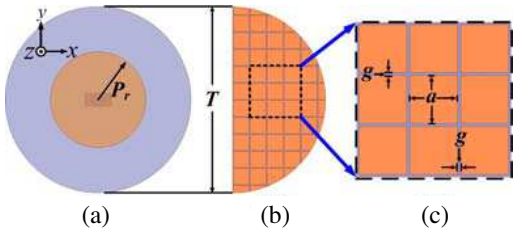

Figure 5: Geometries of (a) patch antenna, (b) MS and (c) unit cell.

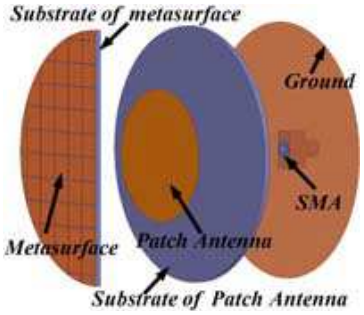

Figure 6: Assembly schematic of PaRMS antenna.

3. SIMULATION AND MEASUREMENT RESULTS

3.1. Frequency Reconfigurable Antenna

The frequency reconfigurability of the FRMS antenna is studied using reflection coefficient S_{11}. The simulated and measured S_{11} of the antenna with different rotation angles θ_R are shown in Fig. 7. The resonant frequency is proportional to the rotation angle. As the rotation angle increases from 10° to 25°, 35°, 55° and 80°, the resonant frequency shifts up from 4.77 GHz to 4.9, 5.07, 5.31 and 5.51 GHz, respectively, with a fractional tuning range of 14.6%. The simulated and measured efficiencies are shown in Fig. 8. It can be seen that the simulated and measured efficiencies are above 80% at the resonant frequencies.

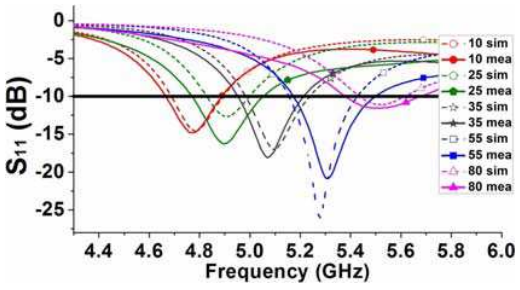

Figure 7: Simulated and measured S_{11} of FRMS antenna with different rotation angles.

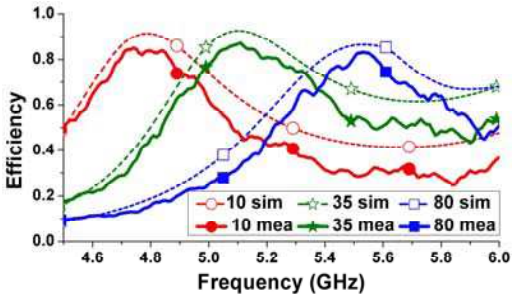

Figure 8: Simulated and measured efficiencies of FRMS antenna.

3.2. Polarization Reconfigurable Antenna

The simulated and measured S_{11} of the PRMS antenna with different rotation angles θ_R are shown in Fig. 9. The impedance bandwidth (for $S_{11} < -10$ dB) in LHCP ($\theta_R = 90°$) and RHCP ($\theta_R = 90°$) are more than from 3–4 GHz as shown in Figs. 9(a) and (c), respectively. In LP, i.e., $\theta_R = 45°$, Fig. 9(b) shows that the simulated and measured frequency bands shift down slightly to 2.82–3.7 GHz and 2.8–3.7 GHz, respectively. However, at $\theta_R = 135°$, Fig. 9(d) shows that the simulated and measured frequency bands shift up slightly to 3.28–4.08 GHz and 3.3–4.05 GHz, respectively.

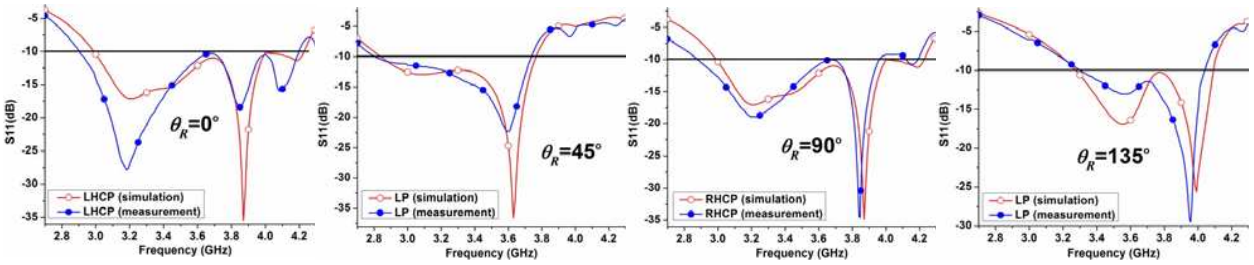

Figure 9: Simulated and measured S_{11} of PRMS antenna for (a) $\theta_R = 0°$, (b) $\theta_R = 45°$, (c) $\theta_R = 90°$ and (b) $\theta_R = 135°$.

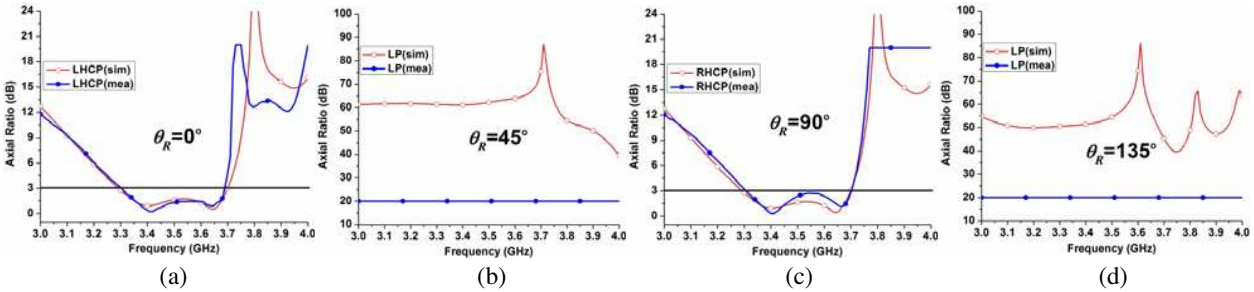

Figure 10: Simulated and measured ARs for different rotation angles.

The simulated and measured axial ratios (ARs) in the boresight of the PRMS antennas (along the $+z$ axis as shown in Fig. 3) are shown in Fig. 10. The simulated and measured ARs are less than 3 dB from 3.3–3.7 GHz for both LHCP and RHCP, with an axial ration bandwidth (ARBW) of 400 MHz (or a fractional bandwidth of 11.4%) as shown in Figs. 10(a) and (c), respectively. With $\theta_R = 45°$ and 135° when the antenna is operated in LP, Figs. 10(b) and (d) show that the simulated ARs are larger than 40 dB from 3–4 GHz, indicating very high linear polarization purity. Since the antenna measurement equipment, Satimo Starlab System, can measure the AR of CP antennas only up to 20 dB, the measured result is therefore a horizontal straight line at 20 dB in Figs. 10(b) and (d).

3.3. Radiation Pattern Reconfigurable Antenna

The simulated S_{11} of the PaRMS antenna is shown as the red line in Fig. 11. Due to the symmetrical antenna structure and the unchanged feeding position, the S_{11} does not vary with the rotation angle. The peak directivity and realized gain are shown in the same figure by the blue lines for the convenience of viewing the operating bandwidth. It can be seen that in the operating bandwidth from 5.48–5.7 GHz (4%), the peak realized gain is above 7 dBi with a peak of 7.7 dBi at 5.6 GHz, where the directivity can reach up to 8.2 dBi. The radiation pattern of the antenna at 5.6 GHz is

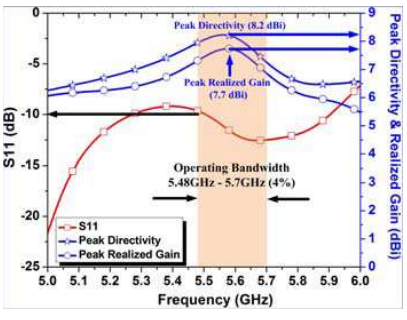

Figure 11: Final operating bandwidth.

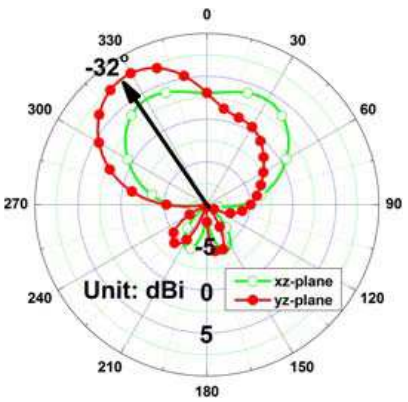

Figure 12: 2D radiation pattern.

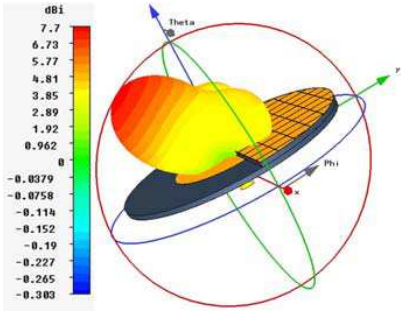

Figure 13: 3D radiation pattern.

shown in Fig. 12. It can be seen that the main beam makes an angle of 32° with the boresight direction. The 3D radiation pattern is plotted in Fig. 13. It can be seen that the main beam is tilted towards to the opposite side of the MS. Thus, the main beam can be steered continuously by rotating the MS around the center of the antenna.

4. CONCLUSIONS

Three different types of reconfigurable antennas, namely, frequency, polarization and pattern configurations, designed using matesurfaces have been presented. The source antennas of these reconfigurable antennas have circular shapes. Results have shown that, by using different MSs underneath the source antennas, the operating frequency, polarization and radiation pattern of the source antennas can be reconfigured by simply rotating the MS around the center of the source antenna.

REFERENCES

1. Sun, X. L., S. W. Cheung, and T. I. Yuk, "Dual-band monopole antenna with frequency-tunable feature for WiMAX applications," *IEEE Antennas and Wireless Propagation Letters*, Vol. 12, 100–103, 2013.
2. Bernhard, J. T., E. Kiely, and G. Washington, "A smart mechanically actuated two-layer electromagnetically coupled microstrip antenna with variable frequency, bandwidth, and antenna gain," *IEEE Transactions on Antennas and Propagation*, Vol. 49, 597–601, 2001.
3. Holloway, C. L., E. F. Kuester, J. A. Gordon, J. O'Hara, J. Booth, and D. R. Smith, "An overview of the theory and applications of metasurfaces: The two-dimensional equivalents of metamaterials," *IEEE Antennas and Propagation Magazine*, Vol. 54, 10–35, 2012.
4. Zhu, H. L., S. W. Cheung, K. L. Chung, and T. I. Yuk, "Linear-to-circular polarization conversion using metasurface," *IEEE Transactions on Antennas and Propagation*, Vol. 61, 4615–4623, 2013.
5. Zhu, H. L., K. L. Chung, X. L. Sun, S. W. Cheung, and T. I. Yuk, "CP metasurfaced antennas excited by LP sources," *2012 IEEE Antennas and Propagation Society International Symposium (APSURSI)*, 1–2, 2012.
6. Zhu, H., S. Cheung, X. Liu, and T. Yuk, "Design of polarization reconfigurable antenna using metasurface," *IEEE Transactions on Antennas and Propagation*, Vol. PP, No. 99, 1 (pages), 2014.
7. Zhu, H. L., X. H. Liu, S. W. Cheung, and T. I. Yuk, "Frequency-reconfigurable antenna using metasurface," *IEEE Transactions on Antennas and Propagation*, Vol. 62, 80–85, 2014.